ISSN 0016-7029, Geochemistry International, 2007, Vol. 45, No. 5, pp. 490–500. © Pleiades Publishing, Ltd., 2007.
Original Russian Text © O.A. Avchenko, K.V. Chudnenko, V.O. Khudolozhkin, I.A. Aleksandrov, 2007, published in Geokhimiya, 2007, No. 5, pp. 547–558.

Oxidation Potential and the Composition of Metamorphic Fluid as a Solution to the Inverse Problem of Convex Programming

O. A. Avchenko[a], K. V. Chudnenko[b], V. O. Khudolozhkin[a], and I. A. Aleksandrov[a]

[a] *Far East Geological Institute, Far East Division, Russian Academy of Sciences, pr. Stoletiya Vladivostoka 159, Vladivostok, 660022 Russia*
e-mail: sirenevka@mail.ru

[b] *Vinogradov Institute of Geochemistry, Siberian Division, Russian Academy of Sciences, ul. Favorskogo 1a, Irkutsk, 664033 Russia*
e-mail: chud@igc.irk.ru

Received October 7, 2005

Abstract—Using the Selektor-C software program package, oxidation potential and the composition of metamorphogenic fluid were determined for mineral assemblages from nine samples of granulite-grade metamorphic rocks by solving the inverse problems of convex programming. The calculated and real mineral assemblages are in good agreement with respect to the composition and association of minerals, which is compelling evidence for the attainment of chemical equilibrium (minimum of Gibbs free energy) under given *P-T* conditions. Based on the dual solution of the inverse problem, a new approach was proposed for the estimation of the oxidation potential of fluid and mineral assemblages, which can be used to determine oxygen potential for almost any mineral association, independent of the presence of magnetite, ilmenite, or graphite. It was found that magnetite-free mineral associations are characterized by highly reducing conditions corresponding to oxygen potentials close to the CCO buffer. The external metamorphic fluid that was present during granulite-facies metamorphism was probably formed in the graphite stability field. The results of calculations for the model aqueous electrolyte solution–mineral assemblage suggest high SiO_2 solubility in the metamorphogenic fluid. Therefore, the process of granulite metamorphism may be a potent geochemical factor of the redistribution and transportation of silica from lower to upper crustal levels.

DOI: 10.1134/S0016702907050060

INTRODUCTION

Inverse problems of physicochemical modeling are those involving the calculation of some input parameters of a physicochemical system, temperature, pressure, redox potential, acidity–alkalinity conditions, and fluid composition or the thermodynamic properties of components and phases of a multisystem, on the basis of the known phase and component compositions of a mineral assemblage. The solution of inverse problems was theoretically substantiated by Karpov [1]. Baksheev [2] provided a significant contribution to the formulation and solution of various inverse problems by the method of physicochemical modeling in the field of mineral geothermobarometry. Of particular importance was the seminal work of Karpov et al. [3] on the formulation and solution of three inverse problems on the basis of the duality principle. They demonstrated how the dual solutions of inverse problems can be used to calculate the empirical functions of the isobaric–isothermal potentials of minerals and aqueous solution species and the possible composition of an aqueous solution or gas phase, if the mineral composition of the basis subsystems is known. The promising application of the method of convex programming in the solution of problems of metamorphic petrology was illustrated by Avchenko and Chudnenko [4]. The goal of this study was the determination of the oxidation potential of mineral associations and the composition of metamorphogenic fluid through the solution of an inverse problem of convex programming on the basis of the Selektor-C software program package.

THEORETICAL AND METHODIC ASPECTS

1. Main Difference between the Methods of Minimization and Phase Correspondence in the Solution of Inverse Problems

Inverse problems are very common in the petrology of metamorphic and magmatic rocks, and they are traditionally solved by the method of phase correspondence using sets of mineralogical geothermobarometers and fugacity sensors [5, 6]. It should be emphasized that there is a fundamental and important difference between the approaches implemented in the Selektor-C program complex and the method of phase correspondence. While any geothermobarometer or fugacity sensor equation requires the expression of a certain end–member or potential-forming reaction or a series of such reactions and, then, their thermodynamic calculation, Selektor-C operates in a different fashion. It does

not calculate reactions but search for the global minimum of a thermodynamic potential (minimum of Gibbs free energy in the formulation of geothermobarometric problems) within a set of bounds imposed by mass balance equations and nonnegativity conditions for the molar amounts of dependent components, taking into account additional one-sided and two-sided constraints on their contents, calculating (modeling) on this basis a certain mineral assemblage. In its turn, this significantly expands, compared with the method of phase correspondence, the possibilities of estimation of temperature, pressure, fluid phase composition, and the degree of equilibrium in natural mineral systems with and without an aqueous electrolyte solution. For instance, the reaction approach to the estimation of oxidation potential in metamorphic rocks requires a particular potential-controlling reaction with the participation of magnetite, hematite, or ilmenite; consequently, the presence of these minerals in the assemblage under investigation is mandatory. In contrast, the method of minimization allows one to determine the oxidation potential of a mineral assemblage free of magnetite, ilmenite, or hematite. Of course, the input information necessary for the solution of inverse problems by the method of phase correspondence is significantly different from that used in convex programming. High-quality chemical analyses of rocks and minerals and comprehensive characteristics of the compositions of mineral assemblages with approximate estimates of volume fractions of minerals are necessary for the solution of inverse problems on the basis of Selektor-C, whereas the knowledge of the compositions of phases in the mineral association are sufficient for the method of phase correspondence. The advantages of the method of minimization over the traditional "reaction" approach for the analysis of mineral equilibria were discussed by Karpov et al. [7].

2. *Importance of the Duality Principle*

For the following discussion, the conceptual definitions of dependent and independent components should be recalled. Dependent components are components of a certain chemical composition or end-members of a certain stoichiometry which are used as a basis for the description of the compositions and thermodynamic properties of minerals and fluids. In this context, independent components are merely the chemical elements Al, Fe, K, Mn, Na, Si, C, Ca, Mg, Ti, H, and O, whose chemical potentials are calculated on the basis of the duality principle. The electron *e* is also an independent component in an aqueous electrolyte solution.

One characteristic feature of the Selektor-C software program package is that it includes a procedure for the calculation of the chemical potential of independent components (Al, Fe, K, H, O, etc.) on the basis of the duality principle. The duality principle implies that the target function of the primal problem, *G(x)*, attains a minimum value if and only if the target function of the dual problem, *F(x, u)*, reaches a maximum, and the two extrema coincide [1]:

$$\min G(x) = \max F(x, u). \quad (1)$$

Gibbs free energy, $G(x)$, can be written as the function

$$G(x) = x'v, \quad (2)$$

where $v = v_j\ (j \in L)$ is the vector whose elements v_j are the chemical potentials of dependent components j. According to the duality principle, Eq. (1) can be rewritten taking into account Eq. (2) as

$$x'v = b'u. \quad (3)$$

It was shown [1] that u in Eq. (3) is a vector whose element u_i is the chemical potential of an independent component. Therefore, Eq. (3) can be rewritten using conventional thermodynamic notation as

$$\sum_j \mu_j N_j = \sum_i u_i N_i = G(x). \quad (4)$$

In Eq. (4), μ_j and u_i are the chemical potentials of dependent and independent components, respectively; and N_j and N_i are their molar amounts. Thus, the duality principle allows us to convert from the computation of the potentials of dependent components to the computation of the potentials of independent components. Tables 1 and 2 give an example of a dual solution for a gas system consisting of the components C, H, and O, which shows that in fact $RT\sum_j \mu_j N_j = RT\sum_i u_i N_i =$ 50294 cal.

Since O and *e* (electron) are independent components, the oxygen fugacity or the redox potential of a system can be determined from the dual solution. The transition from the known u_i values to the calculation of $\log fO_2$ and Eh can be described in the following way.

It is known that the chemical potential of oxygen in a gas mixture at temperature T is

$$\mu_{O_2} = \mu^0(T) + RT\ln fO_2, \quad (5)$$

where $\mu^0(T)$ is the chemical potential of pure oxygen at a pressure of 1 bar and temperature T, fO_2 is the oxygen fugacity, and R is the gas constant.

Equation (5) can be rewritten in decimal logarithm as

$$(\mu_{O_2}/RT - \mu^0(T)/RT)0.4343 = \log fO_2. \quad (6)$$

On the other hand, $\mu_{O_2}/RT = 2u_O$, where u_O is the reduced chemical potential of oxygen obtained from the dual solution of Selektor as the potential of an independent component shown in Table 1 (column 3). Thus, for the example given in Table 1,

$$\log fO_2 = (-58.436 + 38713/RT)0.4343$$
$$= (-58.436 + 19.23)0.4343 = -17.03.$$

The redox potential of the system can be expressed in a similar way. Eh is a simple function of temperature,

Table 1. Characteristics of independent components in the C–H–O system at T = 740°C and P_s = 6200 bar

Independent component	Initial composition (N_j), mole	Residual of mass balance	Reduced chemical potential (u_j)	RTN_ju_j, cal
	1	2	3	4
C	0.110	–6.1446e-14	–1.093361	–242.118
H	1.349	5.5559e-11	–3.832433	–10407.8
O	0.674	1.9516e-11	–29.217961	–39644.36
				Σ = 50294.3

Table 2. Characteristics of dependent components in the C–H–O system at T = 740°C and P_s = 6200 bar

Dependent component	Composition (N_i), mole	$\mu^0(T)$, cal	$RT\ln f_i$	$RTN_i\mu_i$, cal
	1	2	3	4
H_2	0.006793	–25992	10558.8	–104.84
H_2O	0.5618	–91346	17042.7	–41743
CO	0.00157	–70388	9360.6	–95.81
CO_2	0.05507	–136254	16400	–6601
CH_4	0.05290	–49769	16702	–1749
				Σ = 50293.6

pressure, and the reduced chemical potential of an independent component, electron, as a dual solution constrained by the charge balance in the system [8]:

$$\mathrm{Eh} = RTu_e/F,$$

where Eh is the oxidation potential of the system, R = 1.9872 cal K^{-1} mol^{-1}, F is Faraday's constant equal to 23062 cal V^{-1} mol^{-1}, and u_e is the reduced chemical potential of electron. Thus,

$$\mathrm{Eh} = 0.000086Tu_e(\mathrm{V}).$$

By analogy with $\mathrm{pH} = -\log a_{H^+}$, where a_{H^+} is the activity of H^+, redox potential can also be expressed in the activity units of the dependent component e (electron) in water:

$$pe = \log a_e,$$

where a_e is the activity of electron. Eh and pe are linked by the equation

$$pe = \frac{F}{2.3025RT}\mathrm{Eh} \text{ or } pe = 0.4343u_e.$$

The above expressions allow one to directly calculate the oxidation potential of a system, without invoking more complicated relations connecting Eh and pe with pH and oxygen or hydrogen fugacity values.

The duality principle provides a new approach to the estimation of the redox potential of complex mineral associations, fluid, or solution. For instance, it becomes possible to determine oxygen fugacity in an iron-free system and in mineral equilibria that do not include graphite, magnetite, hematite, or ilmenite. The redox potential of an oxygen-free and hydrogen-free system can also be estimated [8].

3. Importance of Adequate Models of Mineral Solid Solutions for Physicochemical Modeling

The accuracy of the oxidation potential and other physicochemical parameters of a thermodynamic system obtained from the dual solution is eventually controlled by the accuracy of inverse problem solution. The accuracy of inverse problem solution is defined here as agreement of the simulated (calculated) mineral assemblage (in terms of mineral set and chemical compositions) with the observed mineral assemblage under the given chemical composition of the rock (vector b). The experience of modeling shows that such agreement can be achieved only if more or less adequate models of mineral solid solutions are used for the solution of the inverse problem. This is related to the fact that the majority of minerals from metamorphic rocks are complex multicomponent and multisite solid solutions. The formation of such solutions is accompanied by energetic effects, which affects the Gibbs free energy of the whole thermodynamic system. It can be convincingly demonstrated that inverse problems cannot be correctly solved on the basis of simple ideal single-site models of solid solutions. In this study, inverse problems were solved using solid solution models for garnet, orthopyroxene, biotite, clinopyroxene, cordierite, olivine, amphibole, ilmenite, staurolite, and epidote after [9], plagioclase after [6], alkali feldspar after [10], and muscovite after [11]. Small corrections were introduced for the calculation of the activity coefficients of pyroxene, amphibole, and ilmenite solid solutions. These models and corrections will be considered in a special publication. The implementation of solid solution models was performed by us and is a new step in the development of the Selektor-C programming complex. As will be

shown below, the models of solid solutions by Holland and Powell [9, 10] coupled with the thermodynamic database for end members by the same authors [12] provide very good solutions to inverse problems in the field of granulite-facies conditions for amphibole-free mineral assemblages. Somewhat poorer solutions are obtained for calcium-rich, which is related to the inadequacy of the current model of hornblende solid solution. Nonetheless, the experience of modeling shows that satisfactory solutions of inverse problems can also be obtained for such rocks. On the other hand, our calculations indicated that the models of amphibole, muscovite, aluminous pyroxene, cordierite, and ilmenite solid solutions require further refinement.

OXIDATION POTENTIAL AND FLUID COMPOSITION IN THE MINERAL ASSEMBLAGE–COMPRESSED GAS MODEL

Nine samples of granulite-facies metamorphic rocks were selected for modeling. The samples were taken from the Okhotsk and Chogar complexes and the Larba block. The chemical compositions of rocks and minerals, the mineral assemblages, and the *P-T* conditions of their formation were determined for these samples by Avchenko [13, 14]. The rock samples are calcium-poor garnet–orthopyroxene, garnet–cordierite, and garnet–biotite–sillimanite gneisses, gneissic quartzites, and granulites (metapelites) and calcium-rich garnet–amphibole–two-pyroxene schists (metabasic rocks). The contents of SiO_2, Al_2O_3, Fe_2O_3, FeO, MgO, CaO, and Na_2O in these rocks are widely variable (Table 3).

The thermodynamic system that was modeled using Selektor-C consisted of 69 components composing the main observed or possible minerals of granulite-facies metamorphic rocks: quartz, plagioclase, alkali feldspar, biotite, orthopyroxene, clinopyroxene, garnet, cordierite, olivine, amphibole, sillimanite, kyanite, andalusite, ilmenite, magnetite, corundum, sapphirine, graphite, native iron, and rutile. In order to constrain solutions, the following amphibolite-facies minerals were also included: muscovite, epidote, staurolite, zoisite, clinozoisite, and titanite. Fluid was modeled by a gas system consisting of six components: H_2O, CO_2, CH_4, CO, H_2, and O_2. The thermodynamic properties of end-members were calculated using the database of Holland and Powell [12], and those of gas components were taken from the database of Reid et al. [15].

The model included two reservoirs. One of them contained certain amounts of H_2O and carbon. Fluid generated under given *P-T* conditions in the first reservoir was introduced into the second reservoir with a real metamorphic rock (vector b) specified by the molar amounts of the components SiO_2, TiO_2, Al_2O_3, Fe_2O_3, FeO, MnO, MgO, CaO, Na_2O, and K_2O. Vector b was calculated for each sample using the data of Table 3. The rock/fluid weight ratio varied widely from 4 to 200. During modeling the *P-T* parameters and the composition of fluid were varied in such a way as to achieve practically perfect agreement between the set of minerals and the compositions of coexisting minerals in the resulting mineral assemblage in the second reservoir and the real observed mineral assemblage.

It appeared that the oxidation potential of the fluid entering from the first reservoir into the second one was the most important factor for the success of such modeling. When a very small amount of carbon was loaded into the first reservoir together with a certain amount of H_2O, magnetite, ilmenite, or even hematite was always present in model solutions, and the mafic minerals showed lower iron fractions compared with their composition in the natural samples. It was therefore neces-

Table 3. Compositions of metamorphic rocks chosen for modeling

Sample no.	SiO_2	TiO_2	Al_2O_3	Fe_2O_3	FeO	MnO	MgO	CaO	Na_2O	K_2O	P_2O_5	H_2O^+	H_2O^-	LOI	Σ
	1	2	3	4	5	6	7	8	9	10	11	12	13	14	15
10v	45.60	0.25	9.81	3.45	24.84	0.80	8.66	2.16	0.81	0.67	0.06	–	0.22	–	97.33
143	72.88	0.25	9.73	4.71	2.80	0.05	5.94	0.34	0.25	1.00	0.12	–	–	1.53	99.60
73v	64.60	0.22	7.16	0.65	17.94	0.17	6.00	0.31	0.05	0.53	0.26	–	0.06	0.08	98.03
1159/2-a	68.95	0.56	15.56	0.86	3.90	0.08	3.36	1.90	2.45	1.34	0.07	–	0.06	0.64	99.73
39-e	47.62	0.57	9.28	15.20	15.84	0.56	3.37	2.54	0.74	1.07	0.10	–	0.24	1.64	98.77
127-g	65.78	0.55	18.13	3.16	2.46	0.22	2.95	1.46	1.88	1.55	0.11	1.42	0.14	–	99.81
136-e	47.96	1.26	14.84	5.54	9.65	0.27	5.61	10.25	2.58	0.46	0.15	–	–	1.24	99.81
SCh-9/129	46.30	2.25	12.56	6.85	11.00	0.29	6.58	10.51	2.08	0.28	0.33	0.07	–	0.25	99.42
SCh-5/58	44.35	1.47	15.17	5.62	10.81	0.16	8.16	11.09	1.55	0.43	0.19	0.01	–	0.88	99.93

Note: Samples 10v, 143, 73v, 39-e, 127-g, and 136-e were characterized in [13], and samples 1159/2-a, SCh-9/129, and SCh-5/58 are taken from [14].

sary to increase the amount of carbon in the first reservoir, which resulted in a more reduced fluid composition and gradual dissolution of magnetite and ilmenite in mafic silicates, the iron fractions of which increased correspondingly. Eventually, magnetite and sometimes even ilmenite were completely dissolved in mafic silicates, and the set and compositional characteristics of minerals approached those in the natural mineral assemblages. The convergence between the solution and the real composition of mineral assemblages was obtained not only with respect to the set of minerals and iron fractions of silicates but also in plagioclase composition and calcium content in garnet (Tables 4, 5). The volume proportions of minerals in any model assemblage were also close to the real proportions, which were estimated by visual observation.

The amount of carbon added to the system depended on the initial amount of H_2O in the first reservoir and was usually not higher than 0.1–0.3 wt %. Figure 1 gives an example of a solution for sample 127-g, in which a gradual increase in the iron content of garnet and coexisting biotite accompanies an increase in the potential of carbon in the system and a decrease in oxygen fugacity (or an increase in the degree of fluid reduction). The 100Fe/(Fe + Mg) ratio of garnet (70%) and coexisting biotite (37%) from the model garnet–biotite–sillimanite assemblage free of magnetite and ilmenite is practically identical to the compositional characteristics of minerals from the observed natural assemblage (Tables 4, 5), and this solution was obtained at a $\log fO_2$ of –17.5 (Fig. 1). Using the same composition of rock, the same garnet–biotite–sillimanite assemblage can be obtained with a more oxidized fluid, but already with magnetite and ilmenite. An increase in the degree of oxidation of the system results in a decrease in the iron fraction of garnet and biotite in this assemblage, and the iron content of minerals may vary widely at a given rock composition (Fig. 1). Thus, a gradual increase in the degree of oxidation in the model system allowed us to almost exactly reproduce the real compositions of minerals in the observed assemblages and determine unequivocally the oxidation potential in various mineral assemblages independent of the presence of magnetite or ilmenite in them (Table 4).

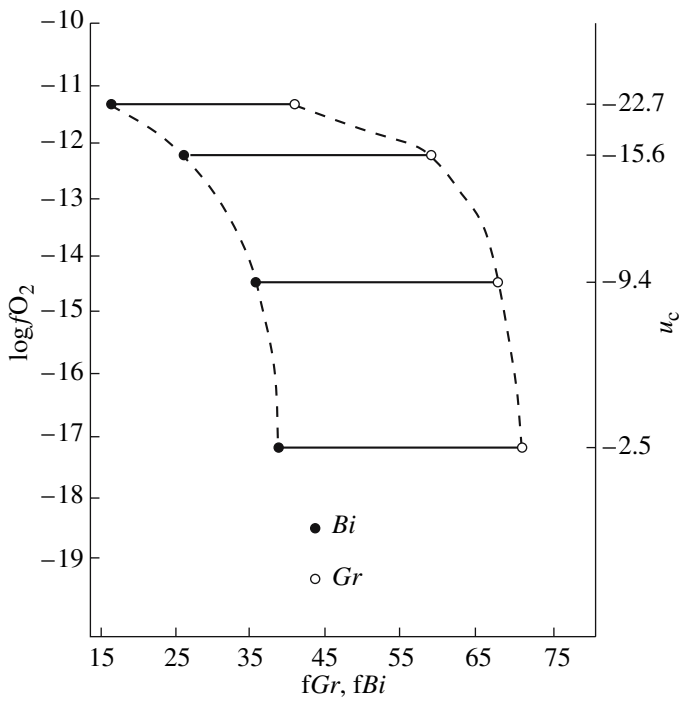

Fig. 1. Variations in the Fe/(Fe + Mg) ratios of garnet (open circles) and biotite (filled circles) as a function of oxygen fugacity ($\log fO_2$) and reduced potential of carbon (u_c). The compositions of coexisting garnet and biotite are connected by tie-lines.

Definite solutions can also be obtained by modeling at a negligible amount of fluid and carbon. The oxidation potential of such assemblages (they do not coincide with the observed natural assemblages in mineral composition) can be referred to as the intrinsic oxidation potential of the rock. It appeared that in all the nine model solutions, the intrinsic oxidation potential of rock is much higher than that determined for the natural assemblage (Table 4). Thus, we obtained evidence for a deficit of reduced gases and free carbon in all the chemical analyses of rocks presented in Table 3.

The results of modeling suggest that all magnetite-free assemblages of metapelitic rocks are strongly reduced and plot in the $\log fO_2 - 10^4/T$K diagram below the quartz–fayalite–magnetite buffer and near the CCO buffer (Fig. 2). The metabasic assemblages with hornblende are more oxidized (Fig. 2). There is another important point concerning the modeling of metabasic assemblages. The observed natural garnet–amphibole–pyroxene assemblages could be reproduced only if, in addition to carbon, a certain amount of CO_2 was added to the system, which decreased H_2O potential. Without such an addition, only pyroxene-free garnet–amphibole–plagioclase–quartz assemblages appeared in the solution. A lower H_2O potential (or a higher CO_2 potential) relative to other mineral assemblages was also necessary for the formation of the biotite-free assemblage of sample 39-e. The model compositions of fluid are shown for all samples in Table 6. It can be seen that the compositions of fluid from all metapelite assemblages (except for sample 39-e) are similar to each other but significantly different from the compositions of fluid in metabasic assemblages.

COMPOSITION OF FLUID IN THE MINERAL ASSEMBLAGE–AQUEOUS ELECTROLYTE SOLUTION MODEL

The thermodynamic system of this model is a perfect analog of that described above except for the addi-

Table 4. (1) Observed and (2) model mineral assemblages under given *P-T* parameters

Sample no.	No.	Mineral assemblage	P_s, bar	T, °C	$\log fO_2^{I}$	$\log fO_2^{II}$	$\log fO_2^{II}$	$\log fO_2^{IV}$
	1	2	3	4	5	6	7	8
10v	1	*Gr + Opx + Pl + Bi + Q**	6200	740	–16.9	–17	–12.7	–17
	2	$Gr_{22} + Opx_{52} + Pl_{16} + Bi_{7.8} + Q_{1.1} + Ilm_{0.3}$						
143	1	*Gr + Opx + Pl + Bi + Cord + Q + Rt*	5200	740	–16.7	–17.2	–11.4	–17.2
	2	$Gr_{14} + Opx_{4} + Pl_{3.4} + Bi_{9.3} + Cord_{9} + Q_{59.9} + Rt_{0.2}$						
73v	1	*Gr + Opx + Kfs + Bi + Q + Mt***	5000	700	–17.8	–18	–14	–18
	2	$Gr_{21.9} + Opx_{22.9} + Bi_{4.9} + Kfs_{1.0} + Q_{49} + Ilm_{0.3}$						
1159/2-a	1	*Gr + Pl + Bi + Sill + Kfs + Ilm + Rt** + Q*	7000	750	–16.4	–16.7	–11.6	–16.7
	2	$Gr_{7.7} + Pl_{31.4} + Sill_{4.8} + Kfs_{0.5} + Bi_{11.9} + Q_{43} + Rt_{0.4} + Gph$**						
39-e	1	*Gr + Opx + Kfs + Pl + Q + Mt + Ilm*	6500	710	–13.7	–16.7	–13	–16.7
	2	$Gr_{31.5} + Opx_{15.6} + Kfs_{17.6} + Pl_{0.03} + Q_{24.8} + Mt_{9.6} + Ilm_{0.8}$						
127-g	1	*Gr + Pl + Bi + Sill + Q*	6800	700	–17.5	–17.7	–11.1	–17.8
	2	$Gr_{7.5} + Pl_{24.7} + Sill_{10.5} + Bi_{14.5} + Q_{42.5} + Rt_{0.1}$						
136-e	1	*Gr + Opx + Cpx + Hb + Pl + Q** + Mt + Ilm*	6000	750	–12.6	–16.1	–12.1	–16.8
	2	$Gr_{6.7} + Opx_{3.1} + Cpx_{1.3} + Hb_{48.3} + Pl_{37.6} + Q_{1.4} + Mt_{0.2} + Ilm_{1.2}$						
SCh-9/129	1	*Gr + Opx +Cpx + Hb + Pl + Mt + Ilm*	7500	750	–14.9	–15.6	–11.8	–16.7
	2	$Gr_{19.8} + Opx_{10} + Cpx_{24.7} + Hb_{13.5} + Pl_{28} + Ilm_{3.4}$						
SCh-5/58	1	*Gr + Cpx + Hb + Pl + Mt + Ilm*	12000	900	–9.9	–12.5	–7.7	–13.6
	2	$Gr_{40} + Cpx_{22.7} + Hb_{16} + Pl_{18.6} + Ilm_{2.5}$						

Notes: $\log fO_2^{I}$ is the logarithm of oxygen fugacity for the model mineral assemblage in equilibrium with fluid; $\log fO_2^{II}$ is the logarithm of oxygen fugacity of fluid not reacting with rock; $\log fO_2^{III}$ is the logarithm of the intrinsic oxygen fugacity of rock calculated assuming a negligible amount of fluid; and $\log fO_2^{IV}$ is the logarithm of oxygen fugacity of fluid for the graphite buffer in the H_2O–C system under given *P-T* parameters. Numbers near mineral indexes denote the volume percentages of minerals obtained in the model.

* Mineral abbreviations: *Gr*, garnet; *Opx*, orthopyroxene; *Cpx*, clinopyroxene; *Hb*, hornblende; *Pl*, plagioclase; *Kfs*, alkali feldspar; *Bi*, biotite; *Cord*, cordierite; *Sill*, sillimanite; *Q*, quartz; *Ilm*, ilmenite; *Mt*, magnetite; *Rt*, rutile; and *Gph*, graphite.

** Trace amounts.

Table 5. Comparison of the (1) observed parameters of minerals from natural assemblages with (2) those obtained in the model

Sample no.	X_{Fe}^{Gr}		X_{Fe}^{Opx}		X_{Fe}^{Bi}		X_{An}^{Pl}		X_{Ca}^{Gr}		X_{Fe}^{Cpx}		X_{Fe}^{Hb}	
	1	2	1	2	1	2	1	2	1	2	1	2	1	2
10v	0.82	0.81	0.63	0.61	0.58	0.53	0.40	0.40	0.11	0.12	–	–	–	–
143	0.57	0.56	0.30	0.35	0.27	0.27	0.27	0.30	0.04	0.02	–	–	–	–
73v	0.78	0.76	0.60	0.56	0.50	0.47	–	–	0.013	0.028	–	–	–	–
1159/2-a	0.53–0.57	0.56	–	–	0.18–0.24	0.27	0.29	0.29	0.025–0.027	0.027	–	–	–	–
39-e	0.81	0.82	0.65	0.60	–	–	0.35	0.35	0.16	0.19	–	–	–	–
127-g	0.73	0.70	–	–	0.35	0.37	0.30	0.28	0.06	0.04	–	–	–	–
136-e	0.80	0.80	0.51	0.57	–	–	0.49	0.48	0.20	0.27	0.42	0.41	0.59	0.53
SCh-9/129	0.80	0.80	0.53	0.56	–	–	0.35	0.35	0.18	0.18	0.44	0.40	–*	0.36
SCh-5/58	0.57	0.59	–	–	–	–	0.35	0.35	0.18	0.21	0.31	0.23	–*	0.41

Notes: X_{Fe} is the Fe/(Fe + Mg) ratio of garnet (*Gr*), orthopyroxene (*Opx*), biotite (*Bi*), clinopyroxene (*Cpx*), and hornblende (*Hb*); X_{An}^{Pl} is the anorthite mole fraction of plagioclase; and X_{Ca}^{Gr} is the Ca/(Ca + Mg + Fe + Mn) ratio of garnet.

* No analysis is available.

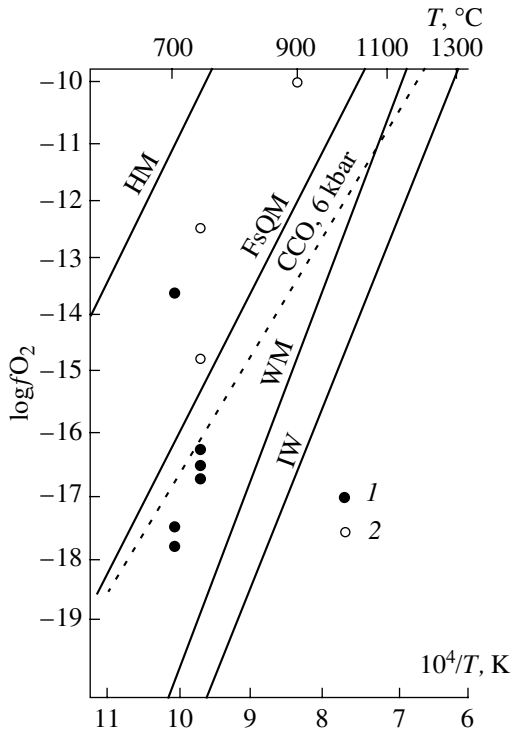

Fig. 2. Mineral assemblages of (*1*) metapelites and (*2*) metabasic rocks on the $\log fO_2 - 10^4/T$ K diagram. Also shown are the lines of buffer equilibria: hematite–magnetite (HM), ferrosilite–quartz–magnetite (FsQM), graphite–carbon oxide (CCO) at 6 kbar, wustite–magnetite (WM), and iron–wustite (IW). The filled circle above the FsQM buffer line is sample 39-e.

tion of 42 dependent components of aqueous electrolyte solution, including the neutral species SiO_2, KOH, NaOH, CH_4, CO_2, O_2, H_2, H_2O, $NaAlO_2$, $NaHSiO_3$, $Al(OH)_3$, $HAlO_2$, $KAlO_2$, $MgCO_3$, $HFeO_2$, FeO, and $CaCO_3$ and the ions K^+, Na^+, H^+, $CaOH^+$, $CaHCO_3^+$, AlO^+, Al^{+3}, Ca^{+2}, Mg^{+2}, Mn^{+2}, Fe^{+2}, Fe^{+3}, $MgHCO_3^+$, $Mg(HCO_3)^+$, $Al(OH)^{+2}$, $Al(OH)_2^+$, AlO_2^-, HCO_3^-, $HSiO_3^-$, CO_3^{-2}, OH^-, $HFeO_2^-$, FeO_2^-, MnO_4^-, and MnO_4^{-2} The thermodynamic properties of aqueous species were described using the databases implemented in Selektor-C (W_Sprons.tdb, W_Shock.tdb, W_Spr 212.tdb, and W_Spr.98.tdb). The activities of ions and neutral species were extrapolated to high *P-T* parameters on the basis of the modified Debye–Hückel equation [17].

Similar to the above calculations, this model consisted of two reservoirs, one of which contained certain amounts of H_2O and C, and the second reservoir included the real composition of metamorphic rock from Table 3. The water–carbon dioxide fluid generated in the first reservoir entered the second reservoir, where it equilibrated with the metamorphic rock. The *P-T* conditions and the degree of fluid reduction were identical to those in the first problem. This allowed us to obtain practically immediately model solutions with mineral sets and compositions identical to those of real mineral assemblages. As can be seen from the solutions presented in Table 7 for four samples, only silicon, sodium, potassium, and aluminum were transported into the solution from the rocks. These elements occur in the fluid as the neutral species SiO_2, KOH, NaOH, and $NaAlO_2$ and the ions $HSiO_3^-$, K^+, Na^+, and AlO_2^-. The fluid is almost free of calcium, magnesium, and iron compounds. Furthermore, the fluid contains significant amounts of carbon dioxide, hydrogen, and, occasionally, methane. It is interesting that the concentration of SiO_2 in the fluid is many times higher than the concentrations of sodium-, potassium-, and aluminum-bearing species (Table 6). In addition, the results of modeling showed that when a water–carbon dioxide fluid interacts with the given mineral assemblages, quartz, albite component of plagioclase, and alkali feldspar were mainly dissolved.

DISCUSSION

In our studies of the mineral association of the Okhotsk complex, it was noted that equilibrium magnetite occurs in these assemblages only in rare peculiar rock varieties with high iron contents [13]. Magnetite was usually absent as an equilibrium phase in ordinary metapelite gneisses with magnesian garnet, cordierite, and sillimanite or biotite and occurred sometimes as a late hysterogenetic mineral. Therefore, the sequences composing the major portion of the Okhotsk complex were in fact "mute" about oxygen potential. However, it has become clear that these magnetite-free rocks could be strongly reduced (Fig. 2), which explains the absence of magnetite in them. As was shown above, the degree of correspondence of model mineral compositions to the observed natural assemblage can be used as a control of oxidation potential for the mineral assemblages of interest (Tables 4, 5). The choice of fluid composition in the first reservoir is in essence arbitrary. The same mineral assemblages can be obtained by reducing water fluid with hydrogen or methane rather than carbon. However, the oxidation potential of given mineral assemblages and equilibrium fluids will be the same at any fluid composition under certain *P-T* conditions, and the solution of the inverse problem is in this sense unequivocal. The choice of the carbon model of fluid is justified by the similarity of model fluid composition from the metapelite gneisses to the results of the gas chromatography of high-temperature extracts from various minerals (Table 6).

Another characteristic feature of the model is that it clearly illustrates the character of oxygen behavior during fluid–rock interaction. If, after obtaining an adequate solution to the inverse problem, the composition of rock is eliminated in the second reservoir, oxidation

Table 6. Contents of H_2O, CO_2, CO, CH_4, and H_2 (wt %) in the model metamorphogenic fluid in equilibrium with the mineral assemblage of rock and the composition of external fluid in minerals according to the data of gas chromatography [16]

Sample no.	H_2O	CO_2	CO	CH_4	H_2	R/W*
	1	2	3	4	5	6
10v	74.2	19.7	0.34	5.6	0.09	9
143	52.9	45.0	0.5	1.4	0.05	50
73v	75.8	20.7	0.2	3.11	0.08	100
1159/2-a	65.2	31.4	0.40	2.9	0.06	200
127-g	91.9	7.3	0.05	0.65	0.05	9
39-e	9.94	90.0	0.01	–	–	20
136-e	17	83	0.01	–	–	20
SCh-9/129	7.0	92.70	0.21	–	–	4
SCh-5/58	7.0	93	0.05	–	–	4
*Hb***	85.35	11.66	0.31	2.51	0.15	–
*Mt***	77.56	19.4	0.46	2.42	0.12	–
*Pl***	75.53	23.16	0.40	0.82	0.09	–

Notes: * Rock/fluid weight ratio accepted for modeling.
** Composition of external fluid according to the data of gas chromatography in hornblende (*Hb*), magnetite (*Mt*), and plagioclase (*Pl*) [16].

potential can be calculated for a sort of external fluid not reacting with the rock. A comparison of the oxidation potential of fluid in equilibrium with rock and without reaction with it shows that the inert (in the sense of D.S. Korzhinskii) behavior of oxygen is characteristic of all magnetite-bearing mineral assemblages, because these rocks evidently buffer the oxygen potential of fluid (Table 4, samples 39-e, 136-e, SCh–9/129, and SCh-5/58). In contrast, the behavior of oxygen in the magnetite-free assemblages of this model approaches a perfectly mobile one because fluid in equilibrium with these rocks is not much different in oxygen potential from the external fluid (Table 4). Although the occurrence of perfectly mobile oxygen behavior in nature cannot be reliably demonstrated for these examples (because it is only a model!), it can be

Table 7. Contents of selected components in aqueous electrolyte solution (mmol/kg) in the aqueous electrolyte–mineral assemblage model under given *P-T* conditions and various rock/fluid ratios (R/W)

Sample no.	*P*, kbar	*T*, °C	Eh	pH	R/W	KOH^0	$NaOH^0$	CH_4^0	CO_2^0	H_2^0	$NaAlO_2^0$	AlO_2^-	HCO_3^-	$HSiO_3^-$	K^+	Na^+	SiO_2^0
	1	2	3	4	5	6	7	8	9	10	11	12	13	14	15	16	17
10-v	6.2	740	–1.06	7.1	7.5	–	–	4382	6767	2653	–	–	1.25	0.37	0.93	4.1	538
10-v	6.2	740	–1.07	7.1	2.0	–	–	1016	2762	2720	–	–	0.66	0.48	0.76	5.2	541
39-e	6.5	710	–0.80	7.0	70	1.10	0.21	–	45006	10.4	1.6	3.8	6.1	0.16	1.5	9.8	386
39-e	6.5	710	–0.79	7.2	20	0.64	0.12	–	77148	4.1	1.4	3.0	6.5	–	1.4	8.9	338
127-g	6.8	700	–0.90	6.4	8	0.94	0.19	256	2040	1066	2.3	8.8	0.34	0.28	1.3	10	572
127-g	6.8	700	–0.90	6.4	0.8	0.92	0.18	2197	3083	1515	2.1	8.3	0.50	0.26	1.3	9.5	544
136-e	6.0	720	–0.80	7.2	15	–	0.12	–	78257	5.4	1.5	2.7	4.4	–	–	7.7	295
136-e*	6.0	720	–0.78	6.7	4	–	0.25	–	5889	28	1.7	5.1	0.7	0.2	–	7.8	522

* The model mineral assemblage (*Gr* + *Hb* + *Pl* + *Q*) does not correspond to the observed assemblage under the given R/W ratio (Table 4).

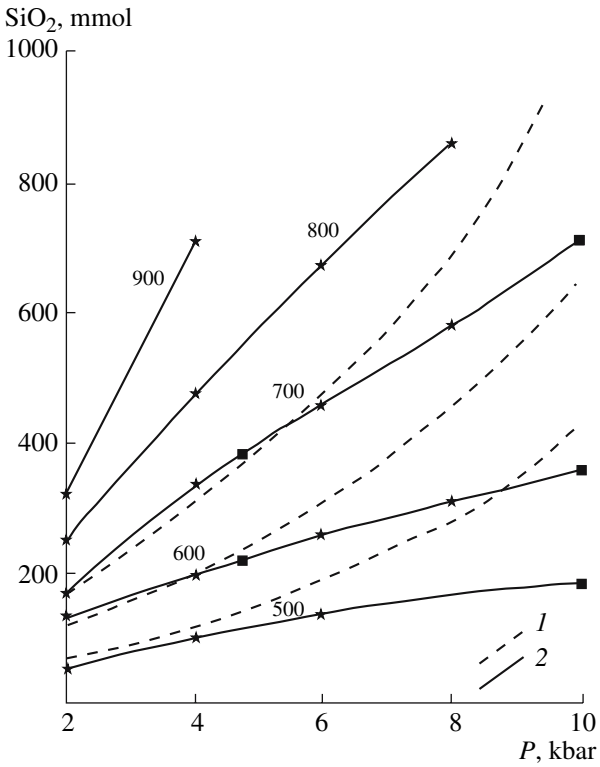

Fig. 3. Comparison of (*1*) experimental SiO_2 solubility in aqueous fluid [19–21] with (*2*) calculated values obtained by Selektor-C. The asterisks on the solid lines show real experiments.

safely suggested that the external metamorphogenic fluid was strongly reduced, and its oxidation potential corresponded to at least the graphite buffer (Table 4). Perhaps, the geochemical profile of the external fluid of the metamorphism of the Okhotsk complex was characterized on a regional scale by the reduced regime approaching the oxygen potential of the CCO buffer (Fig. 2).

The second model (Table 7) clearly shows that a water–carbon dioxide fluid in equilibrium with metamorphic rocks must contain considerable amounts of silica under granulite-facies conditions; if this is the case, high-temperature metamorphism can be an important geochemical factor of extensive SiO_2 transportation from the lower to the upper levels of the Earth's crust. This problem has received little attention in petrological studies concerning geochemical aspects of metamorphism (but not granitization); the redistribution of alkalis rather than silica is usually addressed. Nonetheless, some authors explicitly indicated that metamorphism could be responsible for the removal of considerable amounts of silica [18]. The question is to what extent our model should be believed. The extrapolation of the activity of charged and neutral species to high *P-T* parameters using the HKF equation [17] is reliable only up to 600°C and 5 kbar. There is obviously a need for an experimental check on the accuracy of our calculation. To this end, let us consider experiments on the solubility of quartz, albite, and a mineral assemblage consisting of quartz, andalusite, microcline, and albite.

Figure 3 shows the calculated and experimental isotherms of quartz solubility in pure water. It can be seen that an aqueous fluid in equilibrium with quartz shows high SiO_2 contents (up to hundreds of millimoles per one kilogram of water), and there is good agreement between the calculations and experiments (within ±10–30 mmol) at temperatures of 500–900°C and pressures of 2–6 kbar. The calculated values of SiO_2 solubility become too low at pressures over 6 kbar and temperatures below 700°C. Our model (Table 7) yields SiO_2 solubility from 300 to 600 mmol per one kilogram of water and, as can be seen from Fig. 3 (isotherm 700°C at 6 kbar), is close to the experimental data. The solubility of aluminum and alkalis can be checked by experiments on albite dissolution in pure water [22]. The maximum discrepancy between the calculated and experimental values is observed for aluminum and sodium already at 3.5 kbar (Fig. 4). It is possible that the discrepancy between calculations and experiments is even higher at 6 kbar (region for which our model was developed). However, these data should be interpreted keeping in mind that only a small fraction of the albite component of plagioclase was dissolved in our model (Table 7), and it is therefore unlikely that the calculated concentrations of sodium and aluminum in water–carbon dioxide metamorphogenic fluid are strongly overestimated (underestimated). This suggestion is supported by experimental data [23] on the solubility of the albite–microcline–andalusite–quartz assemblage at 650°C and 2 kbar in acid (pH of 3.5 to 1.2) chloride (KCl + NaCl + HCl) solutions containing 0.01–3 mol/kg Cl, up to 2.05 mol/kg Na, and up to 0.74 mol/kg K at W/R = 2.5–5.0. Our modeling of this experiment showed that the composition of solution was buffered by the mineral assemblage. The calculated concentrations of Si and Al (201 and 0.5 mmol/kg, respectively) in the solution are practically invariant within the whole range of chloride content in the initial solution and coincide with experimental data within the accuracy of chemical analysis. The presented cursory comparison of experimental and calculated data does not claim to be an exhaustive analysis of the problem of verification of the solubility of minerals and rocks calculated by the Selektor-C program package, but it clearly shows that our solubility model for the components of metamorphic rocks is not too far from reality for fluids dominated by water and carbon dioxide. Of course, natural metamorphogenic fluid may contain considerable amounts of chlorine, sulfur, and fluorine, and a more acid fluid composition must result in different estimates for the solubility of rock components [24, 25]. Therefore, our data on the composition of water–carbon dioxide electrolyte under granulite-facies conditions (Table 7) should be regarded as a zero

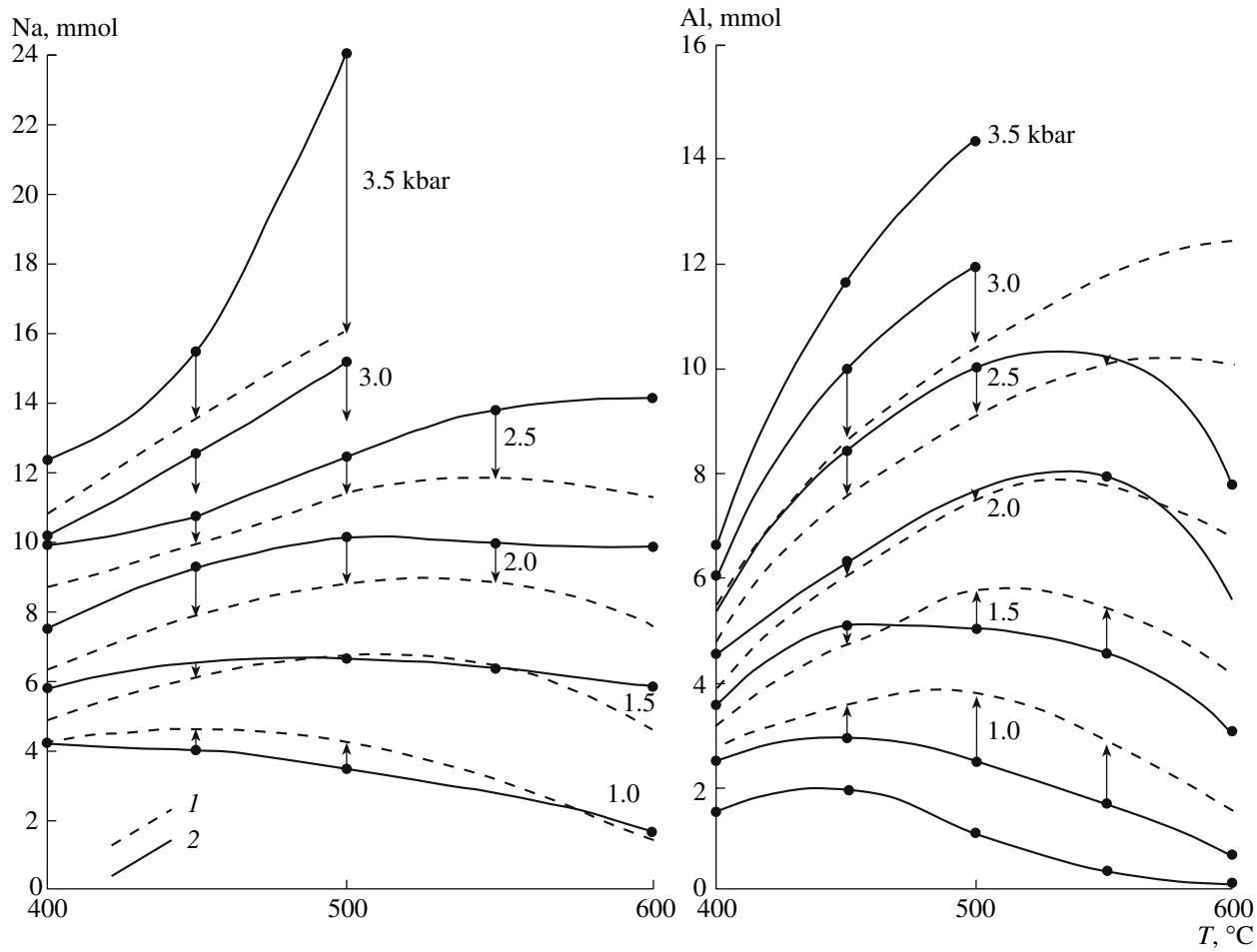

Fig. 4. Comparison of (*1*) experimental albite solubility (for Na and Al) [22] with (*2*) values calculated using Selektor-C. The arrows are drawn to show the degree of convergence between the experimental and calculated isobars.

approximation for the estimation of the concentration and set of aqueous components.

CONCLUSIONS

(1) The agreement between calculated and real mineral assemblages with respect to the compositions and sets of minerals achieved during the solution of inverse problems by convex programming provides compelling evidence that chemical equilibrium was attained under given *P-T* conditions (minimum of Gibbs free energy).

(2) A new approach was proposed for the estimation of the oxidation potential of fluid and mineral assemblages on the basis of the dual solution of an inverse problem. Oxygen potential was estimated for various mineral assemblages of granulite-facies metamorphism independent of the presence of magnetite, ilmenite, or graphite; it was shown that magnetite-free mineral assemblages are strongly reduced and their oxygen potential approaches that of the CCO buffer. It is likely that the external metamorphogenic fluid that accompanied the granulite-facies metamorphism was formed in the graphite stability field.

(3) The results of modeling for the system aqueous electrolyte solution–mineral assemblage indicate high SiO_2 solubility in metamorphogenic fluid. Therefore, the process of granulite metamorphism can be an important geochemical factor of silica redistribution and transportation from the lower to the upper levels of the Earth's crust.

ACKNOWLEDGMENTS

This study was financially supported by integration grant no. 05-2-0-00-001 of the Far East Division, Russian Academy of Sciences, and the Siberian Division, Russian Academy of Sciences.

REFERENCES

1. I. K. Karpov, *Computer-Aided Physicochemical Modeling in Geochemistry* (Nauka, Novosibirsk, 1981) [in Russian].

2. S. A. Baksheev, *Physicochemical Computer Modeling in Geothermobarometry* (Nauka, Novosibirsk, 1991) [in Russian].
3. I. K. Karpov, K. V. Chudnenko, V. A. Bychinskii, and A. S. Bogatyrev, "Solution of Three Inverse Problems in Formulation of Convex Programming," in *Proceedings of International Scientific Conference on Fundamental Problems of Water and Water Resources on the Eve of the Third Millennium, Tomsk, Russia, 2000* (NTL, Tomsk, 2000), pp. 26–29 [in Russian].
4. O. V. Avchenko and K. V. Chudnenko, "Physicochemical Modeling of Mineral Assemblages in Metamorphic Rocks," Dokl. Akad. Nauk **401** (3), 378–383 (2005) [Dokl. Earth Sci. **401**, 398–402 (2005)].
5. L. L. Perchuk and I. D. Ryabchikov, *Phase Correspondence in Mineral Systems* (Nedra, Moscow, 1976) [in Russian].
6. L. Ya. Aranovich, *Mineral Equilibria in Multicomponent Solid Solutions* (Nauka, Moscow, 1991) [in Russian].
7. I. K. Karpov, K. V. Chudnenko, V. A. Bychinskii, et al., "Free Energy Minimization in Calculating Heterogeneous Equilibria," Geol. Geofiz. **36** (4), 3–21 (1995).
8. K. V. Chudnenko, M. V. Artimenko, V. A. Bychinskii, et al., "Calculation of Redox Potential from the Dual Solutions of the Problem of Thermodynamic Modeling as a Convex Programming Problem," in *Proceedings of International Scientific Conference on Fundamental Problems of Water and Water Resources on the Eve of the Third Millennium, Tomsk, Russia, 2000* (NTL, Tomsk, 2000), pp. 448–452 [in Russian].
9. R. Powell and T. Holland, *Source Notes for THERMOCALC Workshorp 2001*. http:/www.earth-sci.unimelb.edu.au/tpg/thermolcalc/
10. R. Powell and T. Holland, "Activity–Composition Relations for Phases in Petrological Calculations: An Asymmetric Multicomponent Formulation," Contrib. Mineral. Petrol. **145**, 492–501 (2003).
11. R. Coggon and T. J. B. Holland, "Mixing Properties of Phengitic Micas and Revised Garnet–Phengite Thermobarometers," J. Metamorph. Geol. **20**, 683–696 (2002).
12. T. J. B. Holland and R. Powell, "An Internally Consistent Thermodynamic Data Set for Phases of Petrological Interest," J. Metamorph. Geol. **16**, 309–343 (1998).
13. O. V. Avchenko, *Petrology of the Okhotsk Metamorphic Complex* (Nauka, Moscow, 1977) [in Russian].
14. O. V. Avchenko, *Mineral Equilibria in Metamorphic Rocks and Problems of Geothermobarometry* (Nauka, Moscow, 1990) [in Russian].
15. R. C. Reid, J. M. Prausnitz, and T. K. Sherwood, *The Properties of Gases and Liquids* (McGraw-Hill Book Company, New York, 1977).
16. O. V. Avchenko, V. O. Khudolozhkin, N. P. Konovalova, and N. N. Barinov, "Carbon-Rich Reduced Fluids of the Sutam Metamorphic Complex," Geochem. Int. **36**, 742–751 (1998).
17. H. C. Helgeson, D. H. Kirkham, and G. C. Flowers, "Theoretical Prediction of the Thermodynamic Behavior of Aqueous Electrolytes at High Pressures and Temperatures; IV. Calculation of Activity Coefficients, Osmotic Coefficients, and Apparent Molal and Standard and Relative Partial Molal Properties to 600°C and 5 Kb," Am. J. Sci. **281**, 1249–1516 (1981).
18. V. A. Buryak, *Metamorphism and Ore Formation* (Nauka, Moscow, 1982) [in Russian].
19. B. M. Mitsuk and L. I. Gorogotskaya, *Physicochemical Transformations of Silica under Metamorphic Conditions* (Naukova Dumka, Kiev, 1980) [in Russian].
20. G. C. Kennedy, "A Portion of the System Silica–Water," Econ. Geol. **45**, 629–653 (1950).
21. C. E. Manning, "Coupled Reaction and Flow in Subduction Zones: Silica Metasomatism in the Mantle Wedge," in *Fluid Flow and Transport in Rocks*, Ed. by B. Jamtveit and W. D. Yardley (Chapman–Hall, London, 1997), pp. 139–148.
22. K. I. Curie, "On the Solubility of Albite in Supercritical Water in the Range 400–600°C and 750–3500 Bars," Am. J. Sci. **266**, 321–341 (1968).
23. T. M. Pak, C. A. Hauzenberger, and L. P. Baumgartner, "Solubility of the Assemblage Albite + K-Feldspar + Andalusite + Quartz in Supercritical Aqueous Chloride Solutions at 650°C and 2 Kbar," Chem. Geol. **200**, 377–393 (2003).
24. B. N. Ryzhenko, S. R. Krainov, and Yu. V. Shvarov, "Physicochemical Factors Forming the Composition of Natural Waters: Verification of the Rock-Water Model," Geokhimiya, No. 6, 630–640 (2003) [Geochem. Int. **41**, 565–575 (2003)].
25. B. N. Ryzhenko, V. L. Barsukov, S. R. Krainov, and Yu. V. Shvarov, "Fluids of the Earth Crust: Chemical Properties (Composition, pH, Eh) and Controlling Factors" in *Symposium on Physicochemical Problems of Endogenous Geologic Processes on the 100th Anniversary of D.S. Korzhinsky, Moscow–Chernogolovka, 1999* (Moscow–Chernogolovka, 1999) [in Russian].